Mycologia Iranica 2025, Vol. 12 (No. 2): 93–104 JIrMS

Original Article

Morpho-phylogenetic characterization of new *Cladosporium* species from Iran

Amirreza Amirmijani[1]✉, Mohammad Javad Pourmoghaddam[2], Zahra Tahmasb Pourafshar[1]

[1]*Department of Plant Protection, Faculty of Agriculture, University of Jiroft, Jiroft, 78671-55311, Iran*
[2]*Department of Plant Protection, Faculty of Agricultural Sciences, University of Guilan, Rasht, Iran*

doi 10.22092/mi.2025.371811.1339

ABSTRACT

The genus *Cladosporium* (*Cladosporiaceae, Dothideomycetes*) is a globally widespread group of fungi, many of which are ecologically and agriculturally important. In Iran, however, the diversity of this genus has been largely overlooked. In this study, fungal samples collected between 2012 and 2024 from dried leaves and plant tissue were investigated. Multiple *Cladosporium* isolates from various Iranian regions were examined using an integrative morpho-phylogenetic approach, combining morphological analyses with molecular phylogenetic studies based on ITS, *act*, and *tef-1α* loci. Our results revealed three species of *Cladosporium*, namely *Cladosporium limoniforme*, *Cladosporium ramotenellum*, and *Cladosporium guizhouense,* which were identified based on morphology, culture characteristics and molecular phylogenetics. This study represents the first report of *Cladosporium guizhouense* in Iran. Comprehensive morphological descriptions, illustrations, and phylogenetic placements are provided for these species.

KEYWORDS

Cladosporiaceae, Iran, molecular phylogeny, morphology, new records.

INTRODUCTION

The genus *Cladosporium* (*Cladosporiaceae, Dothideomycetes*) represents a cosmopolitan and morphologically diverse assemblage of asexual fungi comprising numerous saprobic, endophytic, and pathogenic species (Bensch et al. 2012). These groups of fungi are typically recognized by their dark to olivaceous colonies and the presence of distinctive coronate conidiogenous loci and conidial hila (Lee et al. 2023). Members of this genus occupy a wide range of ecological habitats and are commonly recovered from air, soil, decomposing plant debris, and living plant tissues (Iturrieta-González et al. 2021). While certain *Cladosporium* species are known as important plant pathogens, animal or human opportunistic pathogens, and allergens, others function as key decomposers contributing to nutrient cycling and ecosystem stability (Iturrieta-González et al. 2021). Nevertheless, the taxonomy and delimitation of *Cladosporium* species remain complex and often uncertain, largely due to their overlapping morphological characteristics and the frequent occurrence of cryptic lineages.

Although *Cladosporium* species are widely distributed and functionally diverse, their diversity in Iran has received relatively little attention. Advances in molecular systematics have significantly enhanced species delimitation within the genus, underscoring the importance of integrating morphological traits with molecular data for reliable identification. Over the past decade, research on *Cladosporium* in Iran has gradually expanded (Ershad 2022). Initial investigations provided preliminary insights into its taxonomy and distribution in northern regions, while subsequent studies refined the phylogenetic framework and clarified relationships among Iranian isolates (Amirmijani et al. 2014, 2015). These studies uncovered several previously unreported lineages, highlighting the necessity of further exploration through integrative taxonomic approaches.

Received: 18 Dec. 2025 Revised: 26 Dec. 2025 Accepted: 30 Dec. 2025 Published online: 30 Dec. 2025

✉ Corresponding Author: Amirreza Amirmijani; Email: ar.amirmijani@ujiroft.ac.ir

Published by Iranian Mycological Society (IrMS)—https://mij.areeo.ac.ir

Previous research has documented multiple *Cladosporium* species in Iran, including *C. alicinum, C. cladosporioides, C. delicatulum, C. echinulatum, C. elatum, C. exile, C. iridis, C. halotolerans, C. limoniforme, C. macrocarpum, C. neriicola, C. oxysporum, C. pannosum, C. perangustum, C. pseudocladosporioides, C. scabrellum, C. sphaerospermum, C. tenuissimum*, and *C. uredinicola* among others, from diverse environmental sources (Amirmijani et al. 2014, 2015, Ghiaie Asl et al. 2017, Ayoubi et al. 2017, Ershad 2022). Accurate identification within this genus depends on a combined morpho-phylogenetic framework that merges morphological assessment with molecular analyses (Iturrieta-González et al. 2021, Dai et al. 2025). Molecular identification commonly employs loci such as the internal transcribed spacer (ITS) region of rDNA and partial sequences of the actin (*act*) and translation elongation factor 1-α (*tef-1α*) genes (Iturrieta-González et al. 2021, Dai et al. 2025, Lee et al. 2023). These markers have proven essential for resolving species complexes and detecting novel taxa within *Cladosporium* (Bensch et al. 2010, Schubert et al. 2007).

Expanding upon previous research, the present study aims to address existing knowledge gaps regarding *Cladosporium* diversity in Iran by conducting a comprehensive morpho-phylogenetic assessment of newly detected species from different regions of the country. Using an integrative approach that combines detailed morphological characterization and illustrations with multilocus sequence analyses (ITS, *act*, and *tef-1α*), this work refines the taxonomic placement of Iranian isolates and documents several *Cladosporium* species newly recorded for Iran.

MATERIALS AND METHODS

Isolation and Morphological Study

Fungal samples were collected in recent years (2012–24) from dried leaves and plant tissues, including leaves showing leaf spot symptoms, originating from diverse host species. Isolates were obtained using standard mycological isolation methods and purified by the single-spore method (Ho and Ko, 1991). For morphological assessments, the purified cultures were grown on Malt Extract Agar (MEA, Merck), Oatmeal Agar (OA, Merck), Potato Dextrose Agar (PDA, Merck) and Synthetic Nutrient-poor Agar (SNA: KH2PO4 1gr, KNO3 1gr, MgSO4. 7H2O 0.5gr, KCl 0.5gr, Glucose 0.2gr, Saccharose 0.2gr, Agar 20gr, Distilled Water 1L.) media at 25 °C. After a 10-day incubation period, microscopic mounts were prepared from colonies developed on SNA. Detailed observations were made on colony characteristics—such as pigmentation and growth rates on different media—as well as the morphology, pigmentation, surface ornamentation, and measurements of intercalary and terminal conidia, as well as ramoconidia. Conidiophores and conidiogenous cells features were also documented. Species-level identification was achieved by integrating these morphological observations with relevant literature (Bensch et al. 2012), and species descriptions were prepared.

Molecular study

DNA extraction and PCR

Genomic DNA was extracted by first scraping the surface of seven-day-old colonies on PDA media with a sterile loop. Approximately 100 mg of mycelium and conidia from each isolate were placed in a sterile porcelain mortar, mixed with 800 µL of DNA extraction salt buffer (150 mM NaCl, 100 mM Tris, and 50 mM EDTA; pH 7.5–8.0), and thoroughly ground with a sterile pestle. The resulting homogenate was carefully transferred into a sterile 1.5-mL microcentrifuge tube, and DNA extraction was carried out according to the protocol described by Zhong and Steffenson (2001). Subsequently, 10–30 ng of the extracted DNA was used as template in a 25-µL PCR reaction mixture containing 0.2 pmol of each primer, 0.75 U of Taq DNA polymerase, 0.2 mM of each dNTP, 1.5 mM $MgCl_2$, and 1× PCR buffer. Amplifications were performed using the primer sets ITS1/ITS4 for the partial ITS-rDNA region (White et al. 1990), EF1-728F/EF2 for the *tef-1α* gene (Carbone and Kohn 1999, O'Donnell et al. 1998), and ACT-512F/ACT-783R for the *act* gene (Carbone and Kohn 1999). The thermocycling schedule was performed using a peQSTAR 96X thermal cycler (PEQLAB, Germany) and consisted of an initial denaturation at 94 °C for 5 min, followed by 40 cycles of denaturation at 94 °C for 45 s, annealing at 48 °C (52 °C for *tef-1α* and *act*) for 30 s, and extension at 72 °C for 90 s, with a final elongation step at 72 °C for 6 min. To confirm successful amplification, the PCR products were electrophoresed on a 1% agarose gel at 100 V for 40 min. All amplicons were sent to the Pishgam Company (Tehran, Iran) for sequencing.

Phylogenetic Analysis

The raw sequence file was opened in MEGA Ver. 7 (Kumar et al. 2016). Low-quality sequences were trimmed from the ends, ambiguities were resolved and a clean, reliable FASTA sequence was produced. Initial identification of closely related taxa was performed through the Basic Local Alignment Search Tool (BLAST) for each locus (ITS, *act* and *tef-1α*). Reference sequences were obtained from the National Center for Biotechnology Information (NCBI), with particular attention to type sequences as reported in recent taxonomic studies (Bensch et al. 2015, 2018, Wang et al. 2022, Pereira et al. 2024). The phylogenetic dataset comprised 78 *Cladosporium* strains and one outgroup taxon (*Cercospora beticola* CPC 11557) (Table 1). Sequence alignments were performed using the online server implementation of MAFFT Ver. 7.490 (Katoh et al. 2019) and

Table 1. *Cladosporium* sequences used in the phylogenetic analyses. T: ex-type strain. N/A: Not available

Species	Strain numbers	Country	GenBank accession numbers			References
			act	ITS	*tef-1α*	
Cercospora beticola	CPC 11557^T	Italy	AY840458	AY840527	AY840494	Groenewald et al. (2005)
C. aggregatocicatricatum	CBS 140493^T	New Zealand	KT600645	KT600448	KT600547	Bensch et al. (2015)
C. aggregatocicatricatum	CBS 284.84	Netherlands	KT600647	KT600450	KT600549	Bensch et al. (2015)
C. angustisporum	CBS 125983^T	Australia	HM148482	HM147995	HM148236	Bensch et al. (2010)
C. anthropophilum	CBS 140685^T	USA	LN834621	LN834437	LN834533	Sandoval-Denis et al. (2016)
C. anthropophilum	CPC 13235	Australia	HM148520	HM148033	HM148274	Bensch et al. (2010)
C. anthropophilum	CPC 22315	USA	MF473771	MF472921	MF473348	Bensch et al. (2018)
C. anthropophilum	CPC 10142	South Korea	HM148015	HM148256	HM148502	Bensch et al. (2010)
C. anthropophilum	CPC 11131	India	HM148508	HM148021	HM148262	Bensch et al. (2010)
C. anthropophilum	CBS 674.82	Israel	HM148501	HM148014	HM148255	Bensch et al. (2010)
C. anthropophilum	CPC 22393	USA	MF473772	MF472922	MF473349	Bensch et al. (2018)
C. anthropophilum	CBS 122130	Japan	HM148495	HM148008	HM148249	Bensch et al. (2010)
C. aphidis	CBS 132182^T	Germany	JN906998	JN906978	JN906985	Bensch et al. (2010)
C. arthropodii	CBS 124043^T	New Zealand	JN906998	JN906979	JN906985	Bensch et al. (2012)
C. bambusicola	COAD 2256^T	Brazil	MT373125	MZ318433	MT680204	Costa et al. (2022)
C. bambusicola	COAD 2562	Brazil	OP598123	OP535371	OP676082	Pereira et al. (2024)
C. bambusicola	COAD 2565	Brazil	OP598124	OP535372	OP676083	Pereira et al. (2024)
C. bambusicola	COAD 2573	Brazil	OP598121	OP535369	OP676080	Pereira et al. (2024)
C. bambusicola	COAD 3516	Brazil	OR669144	OR666147	OR669145	Pereira et al. (2024)
C. basiinflatum	CBS 822.84^T	Germany	HM148487	HM148000	HM148241	Bensch et al. (2010)
C. chlamydosporiformans	COAD 2571^T	Kenya	OP598126	OP535374	OP676085	Pereira et al. (2024)
C. chlamydosporiformans	COAD 2561	Brazil	OP598122	OP535370	OP676081	Pereira et al. (2024)
C. chlamydosporiformans	COAD 2568	Ethiopia	OP598130	OP535378	OP676089	Pereira et al. (2024)
C. cladosporioides	CBS 112388^T	Germany	HM148490	HM148003	HM148244	Bensch et al. (2010)
C. cladosporioides	CBS 113738	USA	HM148491	HM148004	HM148245	Bensch et al. (2010)
C. cladosporioides	**UJFCC2941**	**Iran**	**PX763366**	**PX766915**	**PX763372**	**This study**
C. compactisporum	AUMC 11366^T	Egypt	OL514010	MN826822	N/A	Moharram et al. (2022)
C. devikae	BRIP 72278a^T	Australia	MZ344212	MZ303808	MZ344193	Prasannath et al. (2021)
C. eucommiae	GUCC 401.1^T	China	OL519775	OL587465	OL504966	Wang et al. (2022)
C. fildesense	ChFC-554^T	N/A	MN233632	JX845290	MN233633	Crous et al. (2019)
C. guizhouense	GUCC 401.7^T	China	OL519780	OL579741	OL504965	Wang et al. (2022)
C. guizhouense	COAD 3471	Ethiopia	OP598134	OP535382	OP676093	Pereira et al. (2024)
C. guizhouense	**UJFCC3117**	**Iran**	**PX763363**	**PX766912**	**PX763369**	**This study**
C. guizhouense	**UJFCC3120**	**Iran**	**PX763364**	**PX766913**	**PX763370**	**This study**
C. guizhouense	**UJFCC3128**	**Iran**	**PX763365**	**PX766914**	**PX763371**	**This study**
C. herbarum	CBS 121621^T	Netherlands	EF679516	EF679363	EF679440	Schubert et al. (2007)
C. herbarum	CPC 12183	Netherlands	EF679521	EF679368	EF679445	Schubert et al. (2007)
C. limoniforme	CBS 140484^T	Egypt	KT600592	KT600397	KT600494	Bensch et al. (2015)
C. limoniforme	CBS 113737	USA	KT600591	KT600396	KT600493	Bensch et al. (2015)
C. limoniforme	CPC 18086	N/A	KT600597	KT600402	KT600499	Bensch et al. (2015)
C. limoniforme	CPC 13923	Cyprus	KT600596	KT600401	KT600498	Bensch et al. (2015)
C. limoniforme	CPC 22394	USA	MF473985	MF473136	MF473564	Bensch et al. (2018)
C. limoniforme	CGMCC 3.18037	China	KX938379	KX938396	KX938413	Ma et al. (2017)
C. limoniforme	DTO 305-G4	Australia	MF473988	MF473139	MF473567	Bensch et al. (2018)
C. limoniforme	**UJFCC2942**	**Iran**	**PX763367**	**PX766916**	**PX763373**	**This study**
C. macrocarpum	CBS 121623^T	USA	EF679529	EF679375	EF679453	Schubert et al. (2007)
C. magnoliigena	MFLUCC 18-1559^T	China	N/A	MK347813	MK340864	Jayasiri et al. (2019)
C. maltirimosum	SFC20230103-M51^T	South Korea	OQ185195	OQ186147	OQ185155	Lee et al. (2023)
C. maltirimosum	SFC20230103-M52	South Korea	OQ185196	OQ186148	OQ185156	Lee et al. (2023)
C. marinum	SFC20230103-M33^T	South Korea	OQ185177	OQ186129	OQ185137	Lee et al. (2023)
C. pernambucoense	URM 8390^T	Brazil	MZ555745	MZ518828	MZ555732	Pereira et al. (2022)
C. prolongatum	CGMCC 3.18036^T	China	KX938377	KX938394	KX938411	Ma et al. (2017)
C. proteacearum	BRIP 72301a^T	Australia	MZ344213	MZ303809	MZ344194	Prasannath et al. (2021)
C. proteacearum	SFC20230103-M53	South Korea	OQ185002	OQ165252	OQ185084	Lee et al. (2023)
C. proteacearum	SFC20230103-M55	South Korea	OQ185004	OQ165254	OQ185086	Lee et al. (2023)
C. puris	COAD 2487^T	Brazil	MK249980	MK253337	MK293777	Freitas et al. (2021)
C. puyae	CBS 274.80A^T	Colombia	KT600614	KT600418	KT600516	Bensch et al. (2015)
C. ramotenellum	CBS 121628^T	Slovenia	EF679538	EF679384	EF679462	Schubert et al. (2007)
C. ramotenellum	CBS 118.24	Italy	KT600617	KT600421	KT600519	Bensch et al. (2015)
C. ramotenellum	CBS 133.29	N/A	KT600618	KT600422	KT600520	Bensch et al. (2015)
C. ramotenellum	CBS 109501	Turkey	KT600616	KT600420	KT600518	Bensch et al. (2015)
C. ramotenellum	CBS 169.54	England	MF474079	AJ300335	MF473652	Wirsel et al. (2002); Bensch et al. (2018)
C. ramotenellum	CPC 11826	USA	KT600623	KT600426	KT600525	Bensch et al. (2015)
C. ramotenellum	CPC 13407	Portugal	KT600628	KT600431	KT600530	Bensch et al. (2015)
C. ramotenellum	CPC 12385	Australia	KT600627	KT600430	KT600529	Bensch et al. (2015)
C. ramotenellum	CPC 13789	Spain	KT600629	KT600432	KT600531	Bensch et al. (2015)
C. ramotenellum	CPC 19119	Denmark	MF474080	MF473230	MF473653	Bensch et al. (2018)
C. ramotenellum	CPC 13792	Spain	KT600630	KT600433	KT600532	Bensch et al. (2015)

Table 1. Continued.

C. ramotenellum	CPC 11395	South Korea	KT600621	KT600424	KT600523	Bensch et al. (2015)
C. ramotenellum	CPC 13798	Spain	KT600632	KT600435	KT600534	Bensch et al. (2015)
C. ramotenellum	**UJFCC2944**	**Iran**	**PX763368**	**PX766917**	**PX763374**	**This study**
C. ribis	GUCC 21244.1^{T}	China	OP863098	OP852666	OP859046	Yang et al. (2023)
C. setoides	COAD 3470^{T}	Ethiopia	OP598131	OP535379	OP676090	Pereira et al. (2024)
C. sinense	CBS 143363^{T}	China	MF474102	MF473252	MF473675	Ma et al. (2017)
C. variabile	CBS 121635^{T}	USA	EF679556	EF679402	EF679480	Schubert et al. (2007)
C. versiforme	CBS 140491^{T}	Iran	KT600613	KT600417	KT600515	Bensch et al. (2015)
C. vignae	CBS 121.25	USA	HM148718	HM148227	HM148473	Bensch et al. (2010)
C. wenganense	GUCC 21220.1^{T}	China	OP863101	OP852682	OP859049	Yang et al. (2023)
C. yunnanense	KUN HKAS 121704^{T}	China	OL466937	OK338502	OL825680	Xu et al. (2021)

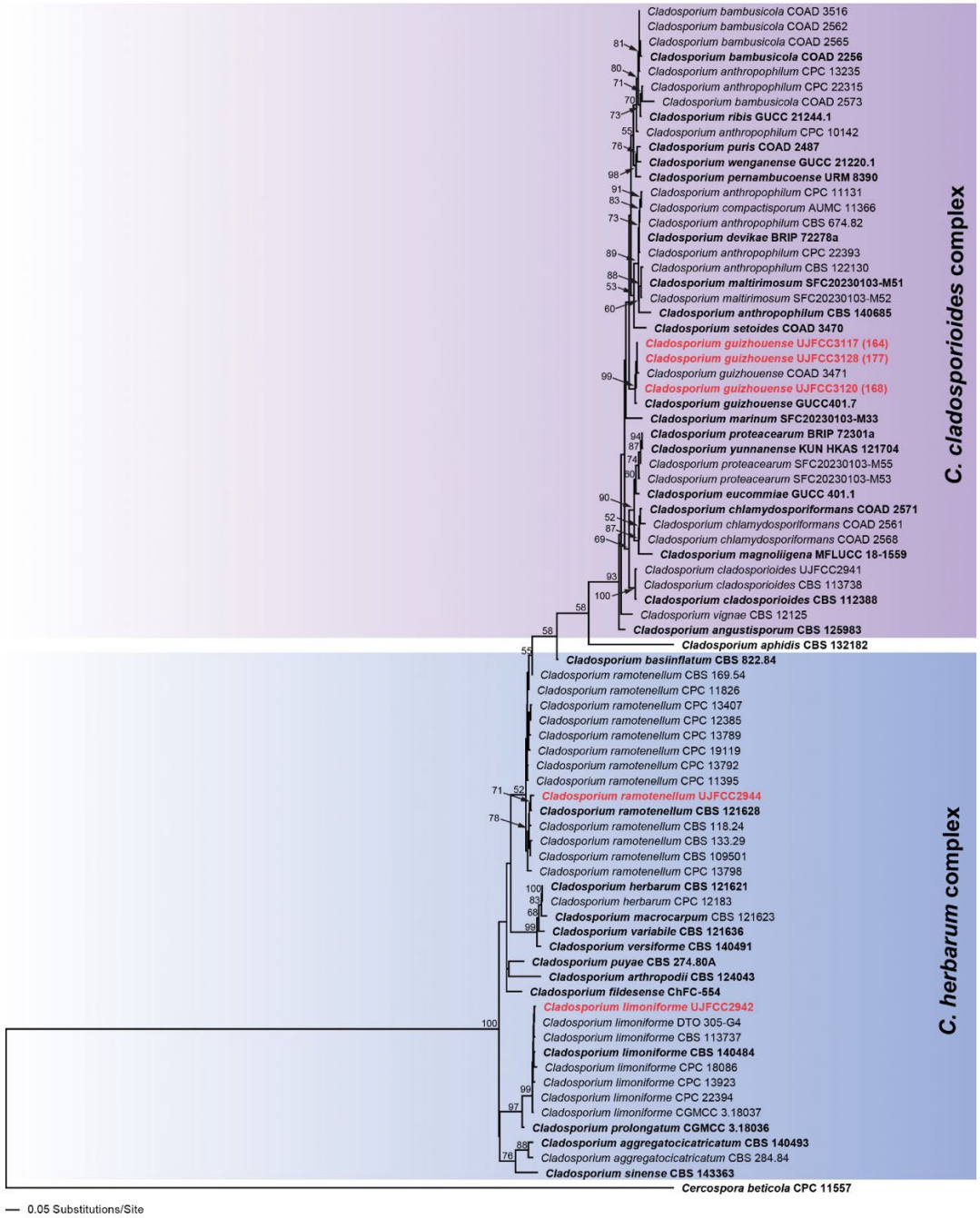

Fig. 1. Phylogram of the best ML trees (lnL = − 7,852.4216) revealed by RAxML from an analysis of the combined ITS-*act-tef-1α* matrix of selected *Cladosporium* species. ML bootstrap support above 50% are given at the branches. *Cercospora beticola* (CPC 11557) was used as outgroup taxon. Strains in bold red were sequenced in the current study. Strains in bold black indicate Type material.

subsequently manually refined in MEGA Ver. 7 (Kumar et al. 2016). Individual gene alignments were concatenated using Mesquite Ver. 3.10 (Maddison and Maddison 2015), yielding a final combined alignment of 1,069 characters (ITS: 461 bp, *act*: 210 bp, *tef-1α*: 398 bp).

Maximum likelihood (ML) analyses were performed with RAxML as implemented in raxmlGUI v. 2.0 (Edler et al. 2021) using the ML + rapid bootstrap setting with 1,000 bootstrap replicates (Felsenstein, 1985) and the GTRGAMMA substitution model. In the Results and Discussion, bootstrap values ≤ 70% are considered low, between 70–90% intermediate and ≥ 90% high. Phylogenetic trees were visualized in PAUP v. 4.0a169 (Swofford 2002) and finalized in Adobe Illustrator® v. CC 2025 (Adobe Inc., San Jose, California, USA).

RESULTES

Phylogeny

The maximum likelihood phylogeny inferred from the combined ITS, *act*, and *tef-1α* dataset resolved the examined *Cladosporium* isolates into well-supported clades corresponding to recognized species and species complexes (Fig. 1). The final alignment comprised 1,069 characters, of which 251 were parsimony informative (30 in ITS, 80 in *act*, and 141 in *tef-1α*). The best-scoring ML tree had a log-likelihood of −7,852.4216. Estimated base frequencies were as follows: A = 0.226885, C = 0.31447, G = 0.246763, T = 0.211881, with substitution rates AC = 1.000717, AG = 3.983449, AT = 1.589382, CG = 1.003971, CT = 3.308326, GT = 1.000000.

Isolates identified as *Cladosporium guizhouense* formed a strongly supported monophyletic clade (ML bootstrap = 99) together with reference strains of the species. Iranian isolates clustered tightly with authenticated strains, showing short branch lengths and no evidence of phylogenetic subdivision. Isolates of *Cladosporium ramotenellum* were resolved as a distinct clade within the *C. herbarum* species complex. The Iranian isolate grouped with multiple reference strains, with moderate to high bootstrap support across internal nodes. The clade was clearly separated from other members of the *herbarum* complex. Similarly, *Cladosporium limoniforme* formed a well-supported monophyletic lineage (ML bootstrap = 99) within the *C. herbarum* species complex. The Iranian isolate clustered with ex-type and reference strains, exhibiting minimal genetic divergence and clear separation from other closely related taxa. Overall, the multilocus phylogeny recovered three distinct and well-supported lineages corresponding to *C. guizhouense*, *C. ramotenellum*, and *C. limoniforme*, confirming their species-level identity and placement within the *C. cladosporioides* and *C. herbarum* species complexes.

Taxonomy

Cladosporium guizhouense S.Y. Wang, Yong Wang bis & Yan Li, MycoKeys 91: 160 (2022). Fig. 2

Colonies on MEA reaching approximately 38 mm diam, after 2 weeks at 25 °C, surface smoke-gray to light olive-gray, woolly or felty, with a whitish narrow edge, radially furrowed, reverse olive-brown, sporulation profuse. Colonies on OA reaching 42 mm diam, after 2 weeks at 25 °C, surface smoke-gray to gray-green, woolly, reverse olive-brown, sporulation profuse. Colonies on PDA reaching 50 mm diam, after 2 weeks at 25 °C, smoke-gray to light olive-gray, woolly, with broad and regular margin, reverse olive-brown, sporulation profuse.

On SNA mycelia abundant, submerged, branched, septate, subhyaline, pale olive-green to olive-green, smooth 1–4 (–4.5) µm, wide. Conidiophores erect, macronematous, branched, septate, light olive-green, smooth, rarely whit unilateral swelling, 53–97 × 3–4 (–4.5) µm. Conidiogenous cell integrates, cylendrical-ablong, 6–36 × 2.5–4 µm. Secondary ramoconidia ellipsoid to cylindrical or subcylindrical, smooth, aseptate or rarely with 1-septate, (5–) 6–24 (–25) × 2–4 µm. Conidia catenate, in simple or branched acropetal chains, variable in size and shape, smooth, and thin-walled, light olive. Terminal conidia: aseptate, ellipsoid to ellipsoid-ovoid, subglobose, 3–5 × 2–2.5 µm. Intercalary conidia: aseptate, fusiform, ellipsoid, avoid, 4–6.5 (–7.5) × 2–3 (–4) µm. Microcyclic conidiogenesis not observed (Fig. 2).

Specimens examined: Iran, Guilan Province, Rasht, on unidentified dried leaves on the ground, 1st December 2012, A.R. Amirmijani (UJFCC3117); Guilan Province, Rasht, on air, 6 May 2013, A.R. Amirmijani (UJFCC3120); Kerman Province, Jiroft, on dried cucumber (*Cucumis sativus*) leaves, 11 July 2021, A.R. Amirmijani (UJFCC3128).

Note: The examined isolates closely matched the morphological features of *C. guizhouense* as outlined by Wang et al. (2022). This predominantly saprobic species belongs to the *C. cladosporioides* species complex and shows close morphological affinity to *C. anthropophilum* and *C. cladosporioides*, rendering separation based solely on morphology challenging. However, both *C. cladosporioides* and *C. anthropophilum* typically produce substantially longer conidiophores, reaching up to 250 µm and 500 µm, respectively, which provide a practical diagnostic character for distinguishing these taxa. This is the first report of *C. guizhouense* in the Iranian Funga.

Cladosporium limoniforme Bensch, Crous & U. Braun, Stud. Mycol. 82: 47 (2015). Fig. 3

Colonies on MEA attaining approximately 58 mm diam, after 2 weeks at 25 °C, surface greenish olivaceous to smoke-grey, felty, growth flat with somewhat elevated colony center, radially furrowed, margins regular, reverse olive-brown to black, sporulation profuse. Colonies on OA attaining 60 mm diam, after 2 weeks at 25 °C, surface grey-olivaceous to olivaceous, felty, margins regular, reverse pale

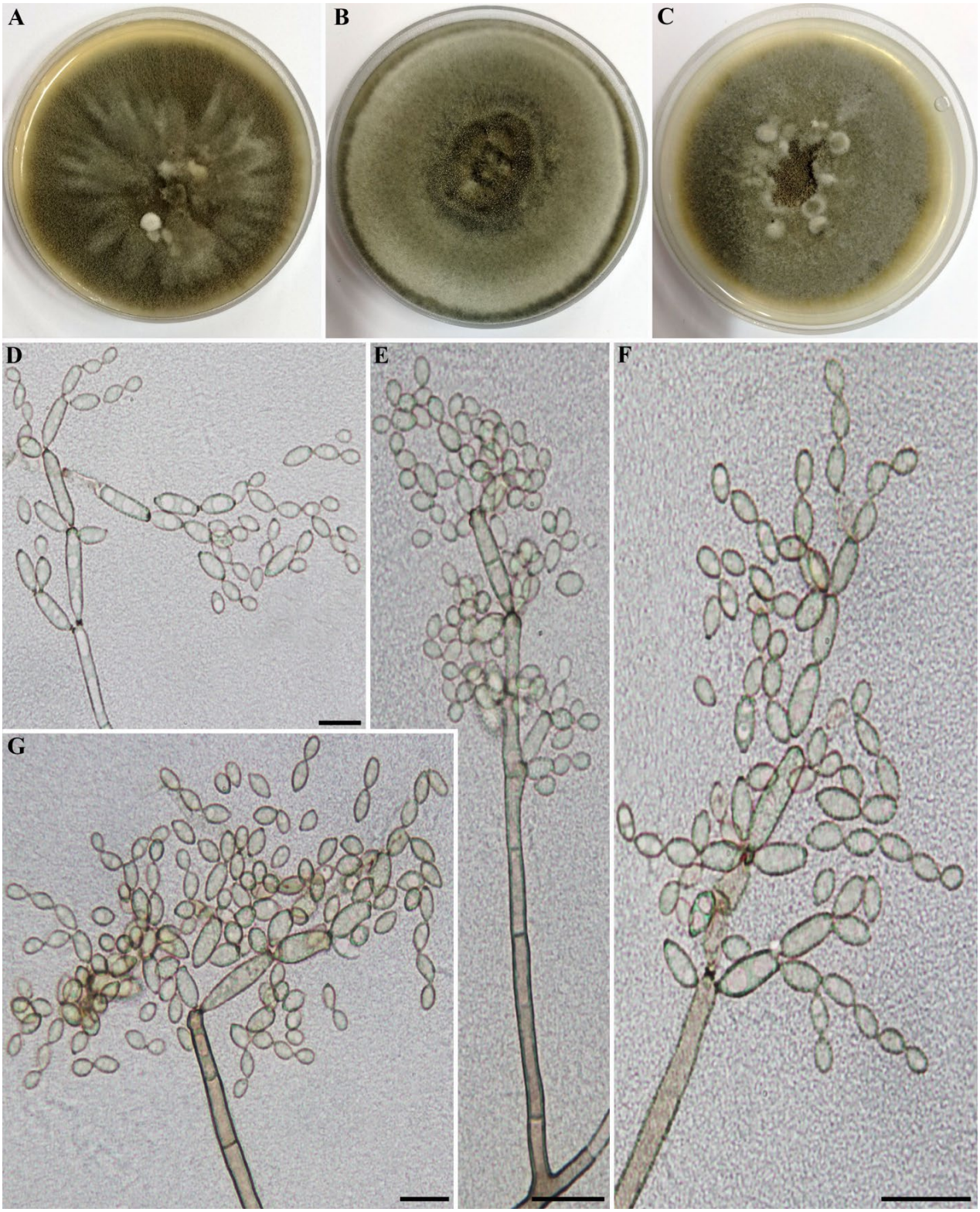

Fig. 2. *Cladosporium guizhouense*. (A–C) 14-day-old colonies incubated at 25 °C on MEA, OA, and PDA, (D–G) Conidiophores, conidiogenous cells, secondary ramoconidia and conidia on SNA. Scale bars: (D–G) 10 µm.

olivaceous-grey to olivaceous-grey, sporulation profuse. Colonies on PDA attaining 50 mm diam, after 2 weeks at 25 °C, smoke-grey to grey-olivaceous, growth low convex, gray-olive to black at edge, both surface and reverse, sporulation profuse.

On SNA, mycelia unbranched, (1–) 2–3 µm wide, pale olivaceous-brown or subhyaline, walls unthickened. Conidiophores solitary, unbranched or rarely with 1-2 branched, macronematous, sometimes semi-macronematous or micronematous, subhyaline,

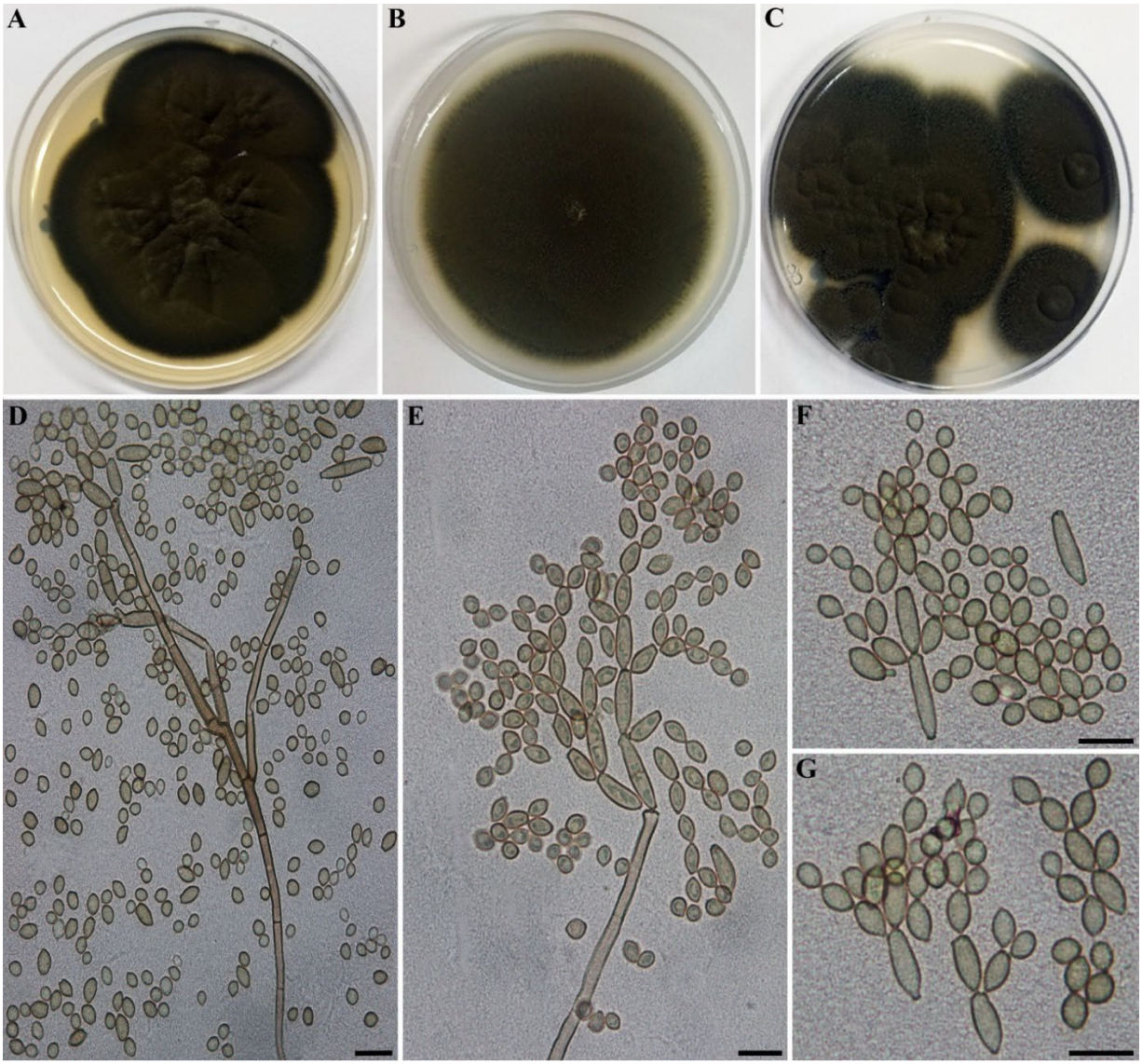

Fig. 3. *Cladosporium limoniforme*. (A–C) 14-day-old colonies incubated at 25 °C on MEA, OA, and PDA, (D–G) Branches of conidiophores, conidiogenous cells, secondary ramoconidia and conidia on SNA. Scale bars: (D–G) 10 µm.

pale brown or pale olivaceous, (11.5–) 22.5–60 (–62) × (2–) 3–4 µm, 1 (–2)-septate. Conidiogenous cells integrate, terminal, rarely intercalary, narrowly cylindrical, subhyaline, 12–45 × 2–3 (–4) µm, with 2–3 (–4) hila at the apex, conidiogenous loci up to 1 µm diam., somewhat thickened. Secondary ramoconidia ellipsoid, cylindrical or subcylindrical, 10–24 × 3–4 µm, 0–1-septate, with (1–) 2–3 distal hila, hila protuberant, up to 1 µm diam, slightly thickened. Conidia catenate, usually up to 6–7 conidia in the terminal unbranched part of the chain, pale olivaceous-brown or pale brown, smooth to loosely verruculose, walls unthickened. Terminal conidia obovoid to subglobose, apex rounded, (2.5–) 3–4 × (2–) 3–4.5 µm, aseptate. Intercalary conidia limoniform, ellipsoid, sometimes fusiform, (3–) 4–8 (–10) × 3–4 (–4.5) µm, aseptate, with 1–3 distal hila. Microcyclic conidiogenesis occasionally occurs (Fig. 3).

Specimen examined: Iran, Kerman Province, Mahan, on dried leaves of Blueberry (*Vaccinium* sect. *Cyanococcus*), 14 December 2024, S. Panahandeh (UJFCC2942).

Note: The examined isolate was morphologically consistent with the description of *Cladosporium limoniforme* provided by Bensch et al. (2015). This species is characterized by the presence of a few micronematous conidiophores, together with distinctive limoniform intercalary conidia. The ornamented conidial surface conforms to features typical of members of the *C. herbarum* species complex. Although *C. limoniforme* is phylogenetically closely allied to *C. aggregatocicatricatum*, the two taxa are readily separable based on morphological characters. In *C. aggregatocicatricatum*, conidiophores are considerably longer and macronematous, bearing clusters of conspicuous scars at apical or intercalary positions. This species was previously reported by Ayubi et al. (2017) as the causal

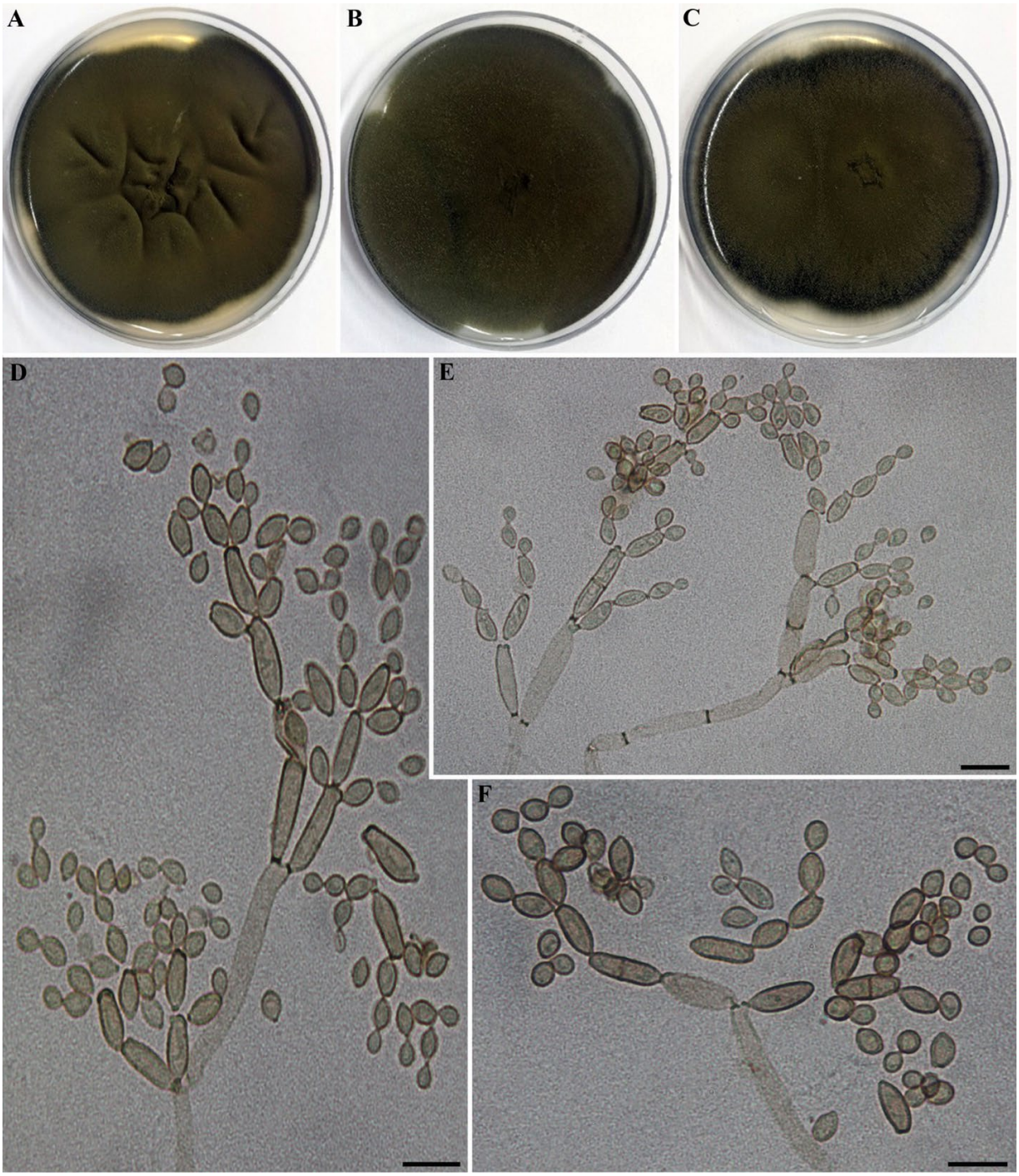

Fig. 4. *Cladosporium ramotenellum*. (A–C) 14-day-old colonies incubated at 25 °C on MEA, OA, and PDA, (D–F) Conidiophores, conidiogenous cells, secondary ramoconidia and branched chain of conidia on SNA. Scale bars: (D–F) 10 µm.

agent of strawberry disease in Iran, and here it is reported for the first time from blueberry (*Vaccinium* sp.) leaves showing blight symptoms in Iran.

Cladosporium ramotenellum K. Schub., Zalar, Crous & U. Braun, Stud. Mycol. 58: 137 (2007). Fig. 4

Colonies on MEA reaching approximately 50 mm diam, after 2 weeks at 25 °C, surface olivaceous - green, felty, radially furrowed, reverse olivaceous-grey to black, sporulation profuse. Colonies on OA reaching 40 mm diam, after 2 weeks at 25 °C, surface grey-olivaceous to olive, felty, reverse olive-brown to black, sporulation profuse. Colonies on PDA reaching 50 mm diam, after 2 weeks at 25 °C, olivaceous to grey-olivaceous, growth low convex, gray-olive to black at edge, both surface and reverse, sporulation profuse.

On SNA mycelia Unbranched, (1–) 2–3 (–4) µm, septate, smooth, subhyaline, walls untickened. Conidiophores solitary, macronematous, straight, unbranched, sometimes branched, subhyaline, (30–) 35–120 × 2.5–3 µm, septate, pale olivaceous or brown, smooth to minutely verruculose, walls unthickened. Conidiogenous cells integrate, terminal, cylindrical, 11–25 × 2–3 (–4) µm, with mostly 2–3 hila, hila protuberant and thickened, 1–1.5 µm diam. Secondary ramoconidia cylindrical or subcylindrical, subhyaline to pale olivaceous, minutely verruculose, (11–) 13–26 × 3–4 (–4.5) µm, 1–2-septate, with 2–3 protuberant hila, 1–1.5 µm diam., somewhat thickened. Conidia catenate, in branched chains, smooth to minutely verruculose. Terminal conidia: globose, ovoid, 2–5 × 2–3 µm, aseptate. Intercalary conidia ellipsoid, pale olivaceous, minutely verruculose, 3–8 (–12) × 3–4 µm, aseptate. Microcyclic conidiogenesis not observed (Fig. 4).

Specimen examined: Iran, Kerman Province, Mahan, on dried leaves of Boysenberry (*Rubus ursinus* x *idaeus*), 20 December 2024, S. Panahandeh (UJFCC2944).

Note: The specimen examined in the present study conforms well to the diagnostic characters of *Cladosporium ramotenellum* described by Schubert et al. (2007). This species was established during their revision of the *C. herbarum* species complex, primarily based on the presence of consistently finely verruculose conidia. Although *C. ramotenellum* is considered saprobic and has been reported from aerial habitats, its overall morphology shows a closer resemblance to *C. cladosporioides*. However, *C. cladosporioides* can be readily distinguished by its smooth-walled conidia, allowing reliable separation from *C. ramotenellum*. This species was recently reported from sugarcane by Asgari et al. (2019) and an endophyte from the *Asteraceae* family by Hatamzadeh et al. (2020) in Iran, but without providing any description. The present description is the first report of this species from Boysenberry (*Rubus ursinus* x *idaeus*) in Iran.

DISCUSSION

Species delimitation in *Cladosporium* remains challenging due to extensive morphological overlap and the presence of multiple cryptic lineages. By applying an integrative morpho-phylogenetic approach, this study clarifies the taxonomic placement of three *Cladosporium* species newly recorded from Iran and provides additional evidence for the robustness of the species-complex concept in this genus.

The combined ITS, *act*, and *tef-1α* dataset yielded strong phylogenetic resolution, with 251 parsimony-informative characters out of 1,069 aligned positions. Consistent with previous studies, *tef-1α* contributed the highest phylogenetic signal, whereas ITS alone showed limited discriminatory power. The maximum likelihood phylogeny recovered three well-supported clades corresponding to the studied isolates, each nested within established *Cladosporium* species complexes. Both *C. limoniforme* and *C. ramotenellum* were resolved within the *C. herbarum* species complex. This placement agrees with the species-complex framework proposed by Bensch et al. (2012, 2015), who emphasized conidial ornamentation as a key diagnostic feature of the *herbarum* lineage. In *C. ramotenellum*, the strongly ornamented conidia are fully congruent with this concept, whereas *C. limoniforme* is distinguished within the same complex by its characteristic lemon-shaped intercalary conidia, highlighting the morphological heterogeneity that can occur within a single evolutionary lineage. Similar intracomplex morphological variation has been documented by Sandoval-Denis et al. (2016), who demonstrated that subtle but stable conidial characters remain taxonomically informative when interpreted in a multilocus phylogenetic context. *Cladosporium guizhouense* was placed within the *C. cladosporioides* species complex and showed a close phylogenetic affinity to *C. anthropophilum*. This result is consistent with earlier multilocus phylogenies presented by Bensch et al. (2012) and later refined by Sandoval-Denis et al. (2016), which recognized *C. anthropophilum* and allied taxa as a distinct lineage characterized by relatively smooth conidia and broad ecological tolerance. The recovery of *C. guizhouense* in Iran considerably extends its known distribution and supports the notion of a wide ecological amplitude within this complex.

Overall, the strong agreement between morphological characteristics, species-complex assignment, and multilocus phylogenetic placement observed in this study supports the current taxonomic framework of *Cladosporium*. These results underscore the previously underestimated diversity of the genus in Iran and confirm that integrative taxonomic approaches are essential for accurately resolving species boundaries within this morphologically conserved group.

ACKNOWLEDGMENT

The authors express their gratitude to Mr. S. Panahandeh for providing the isolates from Blueberry and Boysenberry, and to Ms. Kezhal Zaeri for performing some of the PCR reactions.

AUTHOR CONTRIBUTION

AA: Conceptualization, identification of the isolates, writing – original draft preparation, review and editing; **MJP:** phylogenetic analysis, writing – review and editing; **ZT:** Isolation of the isolates and laboratory works.

DATA AVAILABILITY

Requests for data and materials should be addressed to AR Amirmijani.

DECLARATION

The authors declare no conflicts of interest.

FUNDING

The authors declare that no financial support was received during this research.

ETHICS APPROVAL

This article does not contain any studies with human participants or animals performed by any of the authors.

REFERENCES

Amirmijani AR, Khodaparast SA, and Zare R. 2015. Additions to the knowledge of the genus *Cladosporium* in Iran. Mycologia Iranica. 2(1): 11-21. https://doi.org/10.22043/mi.2015.13654.

Amirmijani AR, Khodaparast SA, and Zare R. 2014. Contribution to the identification of *Cladosporium* species in the North of Iran. Rostaniha. 15(2): 133-145. https://doi.org/10.22092/botany.2014.101237.

Asgari B, Zare R, Taherkhani K, Bakhshi M, Javadi A, Zangeneh S, Moazen H. 2019. Biodiversity of non-mycorrhizal fungi of sugarcane rhizosphere in selected fields of Khuzestan Province. Proceedings of 4th Iranian Mycological Congress; Sari, Iran: p. 27.

Ayoubi N, Soleimani MJ and Zare R. 2017. *Cladosporium* species, a new challenge in strawberry production in Iran. Phytopathologia Mediterranea. 56 (3): 486-493. https://doi.org/10.14601/Phytopathol Mediterr-20151.

Bensch K, Braun U, Groenewald JZ, Crous PW. 2012. The genus *Cladosporium.* Studies in Mycology. 72: 1-401. https://doi.org/10.3114/sim0003.

Bensch K, Groenewald JZ, Braun U, Dijksterhuis J, Yanez-Morales M, Crous PW. 2015. Common but different: The expanding realm of *Cladosporium*. Studies in Mycology. 82(1): 23-74. https://doi.org/ 10.1016/j.simyco.2015.10.001.

Bensch K, Groenewald JZ, Dijksterhuis J, Starink-Willemse M, Andersen B, … et al. 2010. Species and ecological diversity within the *Cladosporium cladosporioides* complex (*Davidiellaceae*, *Capnodiales*). Studies in Mycology. 67: 1-94. https://doi.org/10.3114/sim.2010.67.01.

Bensch K, Groenewald JZ, Meijer M, Dijksterhuis J, Jurjevic Z, … et al. 2018. *Cladosporium* species in indoor environments. Studies in Mycology. 89(1): 177-301.https://doi.org/10.1016/j.simyco.2018.03. 002.

Carbone I. and Kohn LM. 1999. A method for designing primer sets for speciation studies in filamentous ascomycetes. Mycologia. 91: 553-556. https:// doi.org/1 0.1080/00275514.1999.12061051.

Costa PP, Rosado AWC, Pereira OL. 2022. Six new species of *Cladosporium* associated with decayed leaves of native bamboo (*Bambusoideae*) in a fragment of Brazilian Atlantic Forest. Phytotaxa. 560: 1-29. https://doi.org/10.11646/phytotaxa.560.1.1.

Crous PW, Wingfield MJ, Lombard L, Roets F, Swart WJ, … et al. 2019. Fungal Planet description sheets: 951–1041. Persoonia. 43: 223-425. https://doi.org/ 10.3767/persoonia.2019.43.06.

Dai XW, Zhao YL, Cui HX, Cao Y, and Yu, ZF. 2025. *Cladosporium* diversity within seeds of *Allium wallichii* and description of a novel species, *Cladosporium allii-wallichii*. International Journal of Systematic and Evolutionary Microbiology. 75(3): 006730. https://doi.org/10.1099/ijsem.0.006730

Edler D, Klein J, Antonelli A. and Silvestro D. 2021. RaxmlGUI 2.0: A graphical interface and toolkit for phylogenetic analyses using RAxML. Methods in Ecology and Evolution. 12: 373-377. https://doi.org/ 10.1111/2041-210X.13512.

Ershad D. 2022. Fungi and fungal analogues of Iran. Ministry of Agriculture, Agricultural Research, Education and Extension Organization, Iranian Research Institute of Plant Protection, Iran. 695 pp.

Felsenstein J. 1985. Confidence limits on phylogenies: An approach using the bootstrap. Evolution. 39(4): 783-791. https://doi.org/10.1111/j.1558-5646.1985. tb00 420. x.

Freitas ML, Gomes AA, Rosado AW, Pereira OL. 2021. *Cladosporium* species from submerged decayed leaves in Brazil, including a new species and new records. Phytotaxa. 482: 223-239. https://doi.org/ 10.11646/ phytotaxa.482.3.1.

Ghiaie Asl I, Motamedi M, Shokuhi GR, Jalalizand N, Farhang A, and Mirhendi H. 2017. Molecular characterization of environmental *Cladosporium* species isolated from Iran. Current medical mycology. 3(1): 1-5. http://doi.org/10.18869/acadpub.cmm.3.1.1.

Groenewald M, Groenewald JZ, Crous PW. 2005. Distinct species exist within the *Cercospora apii* morphotype. Phytopathology. 95: 951-959. https://doi.org/10.1094 / phyto-95-0951.

Hatamzadeh S, Rahnama K, Nasrollahnejad S, Fotouhifar KB, Hemmati K, White JF, and Taliei F. 2020. Isolation and identification of L-asparaginase-producing endophytic fungi from the Asteraceae family plant species of Iran. PeerJ. 8: e8309. http://doi.org/10.7717/peerj.8309.

Ho, W.C. and W.H. Ko. 1997. A simple method for obtaining single-spore isolates of fungi. *Botanical Bulletin of* Academia Sinica. 38: 41-44.

Iturrieta-González I, García D, and Gené J. 2021. Novel species of *Cladosporium* from environmental sources in Spain. MycoKeys. 77: 1-25. https://doi.org/ 10.3897/mycokeys.77.60862

Jayasiri SC, Hyde KD, Jones EBG, McKenzie EHC, Jeewon R, … et al. 2019. Diversity, morphology and molecular phylogeny of Dothideomycetes on decaying wild seed pods and fruits. Mycosphere. 10(1): 1-186. https://doi.org/10.5943/mycosphere /10/1/1.

Katoh K, Rozewicki J, Yamada KD. 2019. MAFFT online service: Multiple sequence alignment, interactive sequence choice and visualization. Briefings in Bioinformatics. 20(4): 1160-1166. https://doi.org/10.1093/bib/bbx108.

Kumar S, Stecher G, Tamura K. 2016. MEGA7: Molecular Evolutionary Genetics Analysis version 7.0 for bigger datasets. Molecular Biology and Evolution. 33: 1870-1874. https://doi.org/ 10.1093/molbev/ msw054.

Lee W, Kim JS, Seo CW, Lee JW, Kim SH, … et al. 2023. Diversity of *Cladosporium* (*Cladosporiales*, *Cladosporiaceae*) species in marine environments and report on five new species. MycoKeys. 98: 87-111. https://doi.org/10.3897/ mycokeys.98.101918.

Ma R, Chen Q, Fan Y, Wang Q, Chen S, Liu X, Cai L, Yao B. 2017. Six new soil-inhabiting *Cladosporium* species from plateaus in China. Mycologia. 109(2): 244-260. https:// doi.org/10.1080/00275514.2017. 1302254.

Maddison WP, Maddison DR. 2015. Mesquite: a modular system for evolutionary analysis. Version 3.10. http://mesquiteproject.org.

Moharram AM, Zohri AN, Hesham AE, Abdel-Raheam HE, Al-Ameen Maher M, ... et al. 2022. Production of cold-active pectinases by three novel *Cladosporium* species isolated from Egypt and application of the most active enzyme. Scientific Reports. 12: 15599. https://doi.org/10.1038/s41598-022-19807-z.

O'Donnell K, Kistler HC, Cigelnik E, Ploetz RC. 1998. Multiple evolutionary origins of the fungus causing Panama disease of banana: concordant evidence from nuclear and mitochondrial gene genealogies. Proceedings of the National Academy of Sciences. 95: 2044-2049.

Pereira CM, Sarmiento SS, Colmán AA, Belachew-Bekele K, Evans HC, Barreto RW. 2024. Mycodiversity in a micro-habitat: twelve *Cladosporium* species, including four new taxa, isolated from uredinia of coffee leaf rust, *Hemileia vastatrix*. Fungal Systematics and Evolution. 14: 9-33. https://doi.org/10.3114/fuse.2024.14.02.

Pereira ML, Carvalho JL, Lima JM, Barbier E, Bernard E, ... et al. 2022. Richness of *Cladosporium* in a tropical bat cave with the description of two new species. Mycological Progress. 21: 345-357. https://doi.org/ 10.1007/s11557-021-01760-2.

Prasannath K, Shivas RG, Galea VJ, Akinsanmi OA. 2021. Novel *Botrytis* and *Cladosporium* species associated with flower diseases of Macadamia in Australia. Journal of Fungi. 7(11): 898. https://doi.org/10.3390/jof7110898

Sandoval-Denis M, Gene J, Sutton DA, Wiederhold NP, Cano-Lira JF, Guarro J. 2016. New species of *Cladosporium* associated with human and animal infections. Persoonia 36(1): 281-298. https://doi.org/ 10.3767/003158516X691951.

Schubert K, Groenewald JZ, Braun U, Dijksterhuis J, Starink M, … et al. 2007. Biodiversity in the *Cladosporium herbarum* complex (*Davidiellaceae*, *Capnodiales*), with standardisation of methods for *Cladosporium* taxonomy and diagnostics. Studies in Mycology. 58: 105-156. https://doi.org/10.3114/ sim.2007.58.05.

Swofford DL. 2002. PAUP* 4.0b10: phylogenetic analysis using parsimony (*and other methods). Sinauer Associates, Sunderland.

Wang S-Y, Wang Y, Li Y. 2022. *Cladosporium* spp. (*Cladosporiaceae*) isolated from *Eucommia ulmoides* in China. MycoKeys. 91: 151-168. https://doi.org/ 10.3897/mycokeys.91.87841.

White TJ, Bruns TD, Lee S, Taylor S. 1990. Amplification and direct sequencing of fungal ribosomal RNA genes for phylogenetics pp: 315–322 In: M.A. Innis D.H., Gelfand J.J. Sninsky, and T.J. White (Eds). PCR - Protocols and Applications - A Laboratory Manual, Academic Press, New York, USA. https://doi.org/10.1016/B978-0-12-372180-8.50042-1

Wirsel SG, Runge-Froböse C, Ahren DG, Kemen E, Oliver RP, Mendgen KW. 2002. Four or more species of *Cladosporium* sympatrically colonize Phragmites australis. Fungal Genetics and Biology. 35(2): 99-113. https://doi.org/10.1006/fgbi.2001.1314.

Xu YX, Shen HW, Bao DF, Luo ZL, Su HY, Hao YE. 2021. Two new species of *Cladosporium* from leaf spots of *Paris polyphylla* in north-western Yunnan Province, China. Biodiversity Data Journal. 9: e77224. https://doi.org/10.3897/BDJ.9.e77224.

Yang Y, Luo W, Zhang W, Mridha MA, Wijesinghe SN, ... et al. 2023. *Cladosporium* species associated with fruit trees in Guizhou Province, China. Journal of Fungi. 9(2): 250. https://doi.org/10.3390/jof9020250.

Zhong S, and Steffenson BJ. 2001. Virulence and molecular diversity in *Cochliobolus sativus*. Phytopathology. 91: 469-476. https://doi.org/ 10.1094/PHYTO.2001.91.5.469.

توصیف ریخت‌شناسی-فیلوژنتیکی گونه‌های جدید *Cladosporium* از ایران

امیررضا امیرمیجانی[1]✉، محمدجواد پورمقدم[2]، زهرا طهماسب پورافشار[1]

۱. گروه گیاهپزشکی، دانشکده کشاورزی، دانشگاه جیرفت، جیرفت، ایران

۲. گروه گیاهپزشکی، دانشکده علوم کشاورزی، دانشگاه گیلان، رشت، ایران

چکیده

جنس *Cladosporium* (*Cladosporiaceae*، *Dothideomycetes*)، قارچی با پراکنش جهانی است که بسیاری از گونه‌های آن از نظر اکولوژیکی و کشاورزی اهمیت دارند. با این حال، تنوع این جنس در ایران به‌طور کامل بررسی نشده است. در این پژوهش، نمونه‌های قارچی جمع‌آوری‌شده در بازه زمانی ۲۰۱۲ تا ۲۰۲۴ از برگ‌ها و بافت‌های گیاهی خشک از مناطق مختلف ایران بر اساس صفات ریخت‌شناسی و واکاوی فیلوژنتیکی بر استفاده از توالی نواحی ژنی ITS، *act* و *tef-1α* بررسی شدند. نتایج ما منجر به شناسایی سه گونه شامل *Cladosporium guizhouense*، *C. ramotenellum* و *C. limoniforme* بر اساس ویژگی‌های ریخت‌شناسی، خصوصیات پرگنه‌ای و داده‌های فیلوژنتیکی شد. این مطالعه نخستین گزارش از *C. guizhouense* در ایران به شمار می‌رود. همچنین توصیف‌های ریخت‌شناسی جامع، تصاویر و جایگاه فیلوژنتیکی این گونه‌ها در این پژوهش ارائه شده است.

کلمات کلیدی: ایران، ریخت‌شناسی، فیلوژنی مولکولی، گزارش‌های جدید، *Cladosporiaceae*.

مکاتبه کننده: امیررضا امیرمیجانی ar.amirmijani@ujiroft.ac.ir

تاریخ دریافت:۱۴۰۴/۰۹/۲۷، تاریخ بازنگری: ۱۴۰۴/۱۰/۰۵، تاریخ پذیرش: ۱۴۰۴/۱۰/۰۹، تاریخ انتشار برخط: ۱۴۰۴/۱۰/۰۹